Modification of the Lipid−Protein Interaction in Human Low-Density Lipoprotein Destabilizes ApoB-100 and Decreases Oxidizability†

Peter M. Abuja,*,‡ Karl Lohner,§ and Ruth Prassl§

Institute of Biochemistry, SFB Biomembrane Research Center, University of Graz, Schubertstrasse 1, A-8010 Graz, Austria, and Institute of Biophysics and X-ray Structure Research, Austrian Academy of Sciences, Steyrergasse 17, A-8010 Graz, Austria

Received July 6, 1998; Revised Manuscript Received January 4, 1999

ABSTRACT: The interactions of the lipid and protein moiety of human low-density lipoprotein (LDL) and their influence on the oxidation behavior of LDL were modified using an amphipathic peptide, melittin, as a probe. The interaction of melittin with the LDL phospholipid surface resulted in a destabilization of apolipoprotein B-100 (apoB-100) as monitored by differential scanning calorimetry, while the characteristics of lipid core melting remained nearly unchanged. Binding of melittin caused a restriction of lipid chain mobility near the glycerol backbone, but not in the middle or near the methyl terminus of the fatty acyl chains as observed by electron paramagnetic resonance. Also, upon melittin addition, the level of copper binding to apoB-100 and the oxidizability of LDL by Cu^{2+} ions were greatly reduced, as indicated by abolished tryptophan fluorescence quenching upon Cu^{2+} binding and, during oxidation, prolongation of the lag phase of oxidation, attenuated consumption of α-tocopherol, and a lowered maximal rate of conjugated diene formation. This reduction of oxidizability could not be reversed by increasing the Cu^{2+} concentration. It is deduced that interaction of Cu^{2+} and α-tocopherol is required for reductive activation of the metal. It can be abolished by interfering with the interactions between apoB-100 and the lipid moiety of LDL which modifies the conformation of LDL and, as a consequence, hinders copper binding to apoB-100.

Human low-density lipoprotein (LDL)[1] is a quasi-spherical molecule consisting mainly of phospholipids, cholesterol esters, and a single large polypeptide chain, apoB-100. LDL has attracted widespread interest as a putative risk factor for the development of atherosclerosis, in particular with respect to its susceptibility to oxidation (reviewed in refs *1* and *2*). Current investigations of LDL oxidation deal predominantly with the influence of lipid composition on its oxidizability; the influence of the protein component and LDL structural organization have elicited much less interest.

Information about the size and shape of LDL has been provided by small-angle X-ray scattering (SAXS) and small-angle neutron scattering (SANS). In previous studies performed in various laboratories, LDL was found to have a diameter between 22 and 28 nm (reviewed in refs *3* and *4*). In addition, a core−shell arrangement of the constituents of LDL was postulated, with the hydrophobic cholesterol esters and triglycerides in the center (core) surrounded by an amphiphilic monolayer of phospholipids, free cholesterol, and apoB-100 (*5*−*7*). Associated with the phospholipid monolayer is α-tocopherol, the main antioxidant contained in LDL, which, in addition, plays an important role in the initiation of copper-induced LDL oxidation (*8*, *9*).

ApoB-100, the major protein component of LDL, is a hydrophobic protein, consisting of a single large polypeptide chain of 4536 amino acid residues with a molar mass of 514 kDa (*10*, *11*). It has been postulated that apoB-100 interacts with the phospholipid shell of LDL in such a way as to "organize" the surface monolayer (*12*). Like several other apolipoproteins, apoB-100 is thought to contain a number of amphipathic α-helices and β-sheets (*13*) with which the protein probably effectuates this organization of the LDL surface. Also, involvement of apoB-100 in the initiation of LDL oxidation, both by providing electrons for the reduction of Cu^{2+} and by binding copper ions in a specific, saturable manner, has been postulated (*14*). A certain role of apoB-100 in solubilizing copper ions within the lipid moiety of LDL is conceivable, as well. Thus, lipid−protein interactions might have important consequences for the oxidation behavior of LDL and the mechanism by which LDL is oxidized. As the protein becomes inevitably modified during oxidation, resulting in a change in the protein conformation (*15*) and degradation of amino acids, e.g., tryptophan (*16*), or sulfhydryl groups (*17*), a varying extent of interaction between apoB-100 and shell lipids may have important consequences for the changes in the oxidizability of LDL

† Supported by the Austrian Science Funds, Projects SFB00709 (P.M.A.) and P11697 (R.P.), and by the European Union, BIOMED 2 CA Project PL 963191.

* Corresponding author. Fax: +43 316 380 9857. E-mail: peter.abuja@kfunigraz.ac.at.

‡ University of Graz.

§ Austrian Academy of Sciences.

[1] Abbreviations: LDL, low-density lipoprotein; SAXS, small-angle X-ray scattering; SANS, small-angle neutron scattering; PBS, phosphate-buffered saline; 5-DSA, 2-(3-carboxypropyl)-4,4-dimethyl-2-tridecyl-oxazolidinyloxyl; 12-DSA, 2-(10-carboxydecyl)-2-hexyl-4,4-dimethyl-3-oxazolidinyloxyl; EDTA, ethylenediaminetetraacetic acid; AAPH, 2,2′-azobis(2-amidinopropane hydrochloride); DSC, differential scanning calorimetry; TEMPO, 2,2,6,6-tetramethyl-1-piperidinine-*N*-oxyl; EPR, electron paramagnetic resonance; $I(h)$, scattering function; $p(r)$, distance distribution function; CD, conjugated dienes; R_i, rate of initiation; V_{max}, maximum rate of propagation.

10.1021/bi981592p CCC: $18.00
Published on Web 02/23/1999

over time. In addition, LDL which becomes trapped in the subendothelial space of the arterial initma undergoes distinct changes (*18*). Conformational changes of apoB-100 are induced in vitro by interaction with matrix components (glycosaminoglycans) and affect the oxidizability by copper ions (*19*). It is, therefore, of considerable interest to determine which role the protein component of LDL plays in modulating its oxidation behavior. Although the biological relevance of transition metal ions for the initiation of LDL lipid peroxidation in vivo is still debated, apart from the discovery of considerable amounts of redox-active copper and iron in atherosclerotic plaque, findings that cell-mediated oxidation relies on the presence of redox-active transition metal ions (*20*), that ceruloplasmin can provide redox-active copper (*21*) under certain conditions [low pH (*22*) or in the presence of peroxynitrite (*23*)], and that activated human monocytes secrete ceruloplasmin (*24*) have sustained interest in this particularly active prooxidant for LDL. Moreover, copper-induced oxidation of LDL is the most widely used model in clinical studies, and there is some correlation between the susceptibility of LDL to oxidation of in vitro and in vivo markers (*25*).

In this study, we used melittin as a probe to investigate the interaction of apoB-100 with the lipid components of LDL, by monitoring the effects on LDL oxidizability and structure. Melittin, the major constituent of bee venom, forms an amphipathic α-helix in bilayer membranes and has the ability to destabilize them (reviewed in ref *26*). On the other hand, some domains of apoB-100 are supposed to stabilize the surface of LDL (*27*). We expected that melittin would preferentially interact with the surface phospholipids of LDL and thus affect the interaction between apoB-100 and the lipid moiety of LDL. We observed that this eventually leads to destabilization of the apoprotein and as a consequence to reduced oxidizability of LDL.

MATERIALS AND METHODS

Reagents. The reagents used were AR grade or better, obtained from Merck or Sigma-Aldrich (Vienna, Austria). Melittin was from Serva and was essentially free of phospholipase A_2 activity, which was assessed in our laboratory by incubation with 1-palmitoyl-2-oleoylphosphatidylcholine at a lipid/peptide molar ratio of 50 for 24 h at 45 °C. Aliquots were taken and analyzed by thin-layer chromatography using $CHCl_3/CH_3OH/NH_{3,conc}$ (65/35/5 v/v) as the solvent. One single spot could be detected by molybdate staining and charring, indicating the integrity of the samples.

Phosphate buffered saline (PBS) was 10 mM sodium phosphate buffer (pH 7.4) containing 0.15 M sodium chloride. The spin-labels, 2-(3-carboxypropyl)-4,4-dimethyl-2-tridecyloxazolidinyloxyl (5-DSA) and 2-(10-carboxydecyl)-2-hexyl-4,4-dimethyl-3-oxazolidinyloxyl (12-DSA), were obtained from Sigma-Aldrich.

Storage of Plasma and Preparation of LDL. EDTA-containing (1 mg/mL) pooled plasma was prepared immediately after obtaining blood of fasted, normolipidemic volunteers (25−35 years old). Sucrose was added to give a final concentration of 0.6%, and then the pool was split into aliquots and stored at −80 °C for a maximum of 6 weeks. It has been shown previously that such storage conditions affect neither the antioxidant concentrations nor the oxidation behavior of LDL prepared from such plasma (*28*). Moreover, DSC experiments with LDL were performed with LDL prepared from fresh and frozen plasma without detectable differences in phase transition and protein unfolding.

LDL was prepared by ultracentrifugation using a single-step discontinuous gradient in a Beckman NTV65 rotor at 60 000 rpm for 2 h at 10 °C as described previously (*28*). The LDL solution was filtered through a 0.22 μm filter adapted to a syringe into a sterile, glass vial (TechneVial, Mallinckrodt-Diagnostica) and stored at 4 °C under argon in the dark for up to 1 week.

Loading of LDL with α-Tocopherol. Pooled EDTA plasma was incubated with ethanolic α-tocopherol (250 mM, 1% of the total plasma volume) at 37 °C under argon in the dark, and LDL was isolated subsequently as described above. As a control, plasma incubated with the same amount of ethanol was used (*29*).

Chemical Analysis. Protein quantitation was performed with the BCA assay using albumin as a standard (Pierce, Rockford, IL). For routine quantitation of LDL, measurement of total cholesterol was performed with the CHOD-PAP enzymatic test kit (Boehringer-Mannheim). The total LDL concentration is expressed in micromolar, assuming a molar mass of 2.5 MDa and a total cholesterol (free and esterified) content of the LDL samples of 31.6 wt % (*29*).

Quantification of α-tocopherol was performed with the method described previously (*9*). Briefly, 1 mL of sample (containing 0.1 nmol of LDL) was withdrawn from the reaction mixture and immediately mixed with the same volume of ice-cold ethanol containing 2 mg/mL butylated hydroxytoluene and 50 μL of an aqueous solution of 100 mg/mL EDTA. Extraction was performed with 1.5 mL of hexane by vortexing for >1 min. HPLC analysis was performed in principle as described previously (*9*), using external standardization.

LDL Oxidation. Before oxidation, a volume of 0.5−1.0 mL of the LDL stock solution was desalted and made EDTA-free by gel filtration in Econo-Pac 10DG columns (Bio-Rad, Richmond, CA) with PBS as the eluting buffer (*28*). The LDL concentration in the PBS solution was then determined by measuring the total amount of cholesterol as described before.

The LDL oxidation process was followed by recording the conjugated diene absorbency at 234 nm (*29*) in a Beckman DU-640 spectrophotometer at 37 °C. Appropriate volumes of the EDTA-free LDL solutions and PBS were pipetted into a set of six quartz cuvettes, and the oxidation process was started by adding an aqueous solution of $CuSO_4$ (final concentration of 1.6 μM) or AAPH [2,2′-azobis(2-amidinopropane hydrochloride)] (final concentration of 1 mM), dissolved in PBS.

Recording of conjugated dienes was started immediately after the addition of $CuSO_4$ or AAPH and continued in intervals of 4−6 min. The recorded absorbency data were converted to molar concentrations of conjugated dienes using a molar absorption coefficient of 29 500 M^{-1} cm^{-1} (in case of AAPH-mediated oxidation, blank AAPH absorbency was subtracted).

Small-Angle X-ray Scattering (SAXS). Small-angle X-ray scattering was measured by an integrated MBG-SAX camera system (HECUS-MBraun, Graz, Austria), based on the Kratky line collimator, equipped with a position sensitive

detector, a Ni-filtered beam-stop system, and an automatic temperature and time programmer and data collection unit. The camera was operated at a rotating anode generator (RU-200B; Rigaku Denki) with CuKα radiation (wavelength of 0.1542 nm).

To 100 μL of LDL solution containing 20 mg/mL LDL in PBS was added 5 μL of an aqueous melittin stock solution (6 mg/mL) to obtain a final melittin concentration of 0.1 mM, corresponding to about 12−13 molecules of melittin per LDL particle and about one melittin per 50 phospholipid molecules, assuming an average of 700 phospholipid molecules per LDL. The measurements were performed at 10 and 37 °C, respectively, with an exposure time of 8 h. No apparent aggregation of LDL due to the length of radiation exposure was noticed in native LDL.

The scattering curves were normalized for integral primary beam intensity; the buffer baseline was subtracted, and the curves were finally normalized for lipoprotein concentration. Deconvolution and inverse Fourier transform of the data obtained with slit collimation were performed using the ITP program (*30*) as described previously (*31*).

Differential Scanning Calorimetry (DSC). Calorimetric experiments were performed with a model DASM-4 high-sensitivity, adiabatic differential scanning microcalorimeter (Biopribor, Pushchino, Russia) at a heating rate of 1 °C/min. The cells were pressurized with nitrogen to about 250 kPa to avoid air bubble formation during high-temperature heating. PBS was used to fill the reference cell. The lipoprotein concentration was about 5 mg/mL throughout all calorimetric experiments. Aliquot amounts of the melittin stock solution (6 mg/mL) were added to give final ratios of 5, 10, and 100 mol of melittin/mol of LDL.

Electron Paramagnetic Resonance (EPR) Measurements. Appropriate amounts of spin-labels (5-DSA and 12-DSA) dissolved in ethanol (the actual label concentration was calibrated with a TEMPO standard) were dried by evaporating the organic solvent under a stream of nitrogen. The dry film was dispersed in about 250 μL of LDL solution (14 μM) and incubated with gentle shaking for 2 h at room temperature in an argon atmosphere. The molar ratio of spin-label to LDL was 7/1. To the spin-labeled LDL preparation was added an aqueous solution of melittin to obtain ratios of 1, 10, and 100 mol of melittin/mol of LDL. As a control, only PBS was added instead of melittin. EPR experiments were performed as described elsewhere (*32*).

Fluorescence Measurements. LDL tryptophan fluorescence decay was measured using a Perkin-Elmer LS-50-B spectrofluorimeter, at 282 and 331 nm (excitation and emission, respectively), as well as spectra (excitation at 282 nm) as described previously (*16*). Samples were thermostated at 37 °C.

RESULTS

Small-Angle X-ray Scattering (SAXS). Panels A and B of Figure 1 show the small-angle X-ray scattering curves, $I(h)$, for LDL at 10 and 37 °C, in the absence and presence of melittin, measured in the angular range of 0.1−2 nm^{-1} [$h = (4\pi \sin\theta)/\lambda$; 2θ = scattering angle; $\lambda = 0.1542$ nm]. Details concerning data evaluation and interpretation of LDL SAXS data of native LDL are described elsewhere (*7*, *31*). The determination of the innermost part of $I(h)$, in particular at

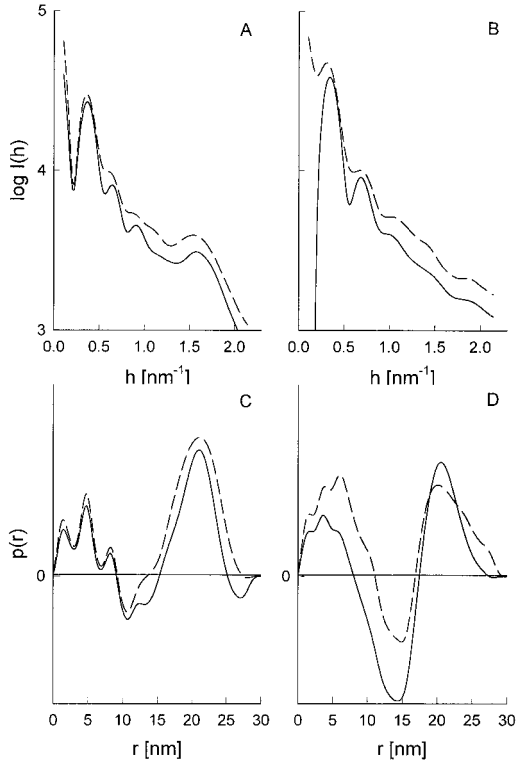

FIGURE 1: Desmeared small-angle X-ray scattering curves $I(h)$ for LDL (solid lines) and LDL treated with melittin at a ratio of about 100 mol of melittin/mol of LDL (dashed lines). The curves for 10 (A) and 37 °C (B) are shown. The values for the corresponding electron pair distance distribution functions $p(r)$ are shown in panels C and D.

37 °C, is notoriously difficult, owing to the low contrast of the central scattering maximum. The corresponding electron pair distance distribution curves, $p(r)$, obtained with indirect Fourier transforms (*30*) are shown in panels C and D of Figure 1. The characteristic maximum of $I(h)$ at $h = 1.7$ nm^{-1}, obtained at 10 °C, resulting from an ordered core lipid arrangement remains unaffected by melittin. This maximum disappeared at 37 °C, due to core-lipid melting, both in the absence and in the presence of melittin. The maximum particle diameter, defined as the distance where $p(r)$ approaches zero, was higher for melittin-treated LDL by about 1 nm. The shift to lower angles of the angular positions of the maxima in $I(h)$, in the presence of melittin, was even more pronounced at 37 °C. Thus, the effects of melittin are directed to the outer layer of the particle, whereas the core remains unaffected.

Differential Scanning Calorimetry (DSC). Upon the mixture being heated from 0 to 40 °C, one endothermic transition was observed, corresponding to the order−disorder transition of the core lipids ("core-lipid melting", Figure 2A) (*5*, *33*). Addition of low concentrations of melittin (up to 10 mol of melittin/mol of LDL) had no influence on the thermotropic core transition temperature ($T_{m,CE} = 27.2$ °C). At higher melittin concentrations, a significant shift of $T_{m,CE}$ to higher temperatures occurred ($T_{m,CE} = 31.1 \pm 0.2$ °C, mean of two independent measurements).

The main impact of melittin was observed with respect to the thermotropic unfolding characteristics of apoB-100 (Figure 2B). In native LDL, denaturation of apoB-100 occurred in a single, irreversible step, at approximately 80 °C (*5*). Even low concentrations of melittin (5 mol/mol of

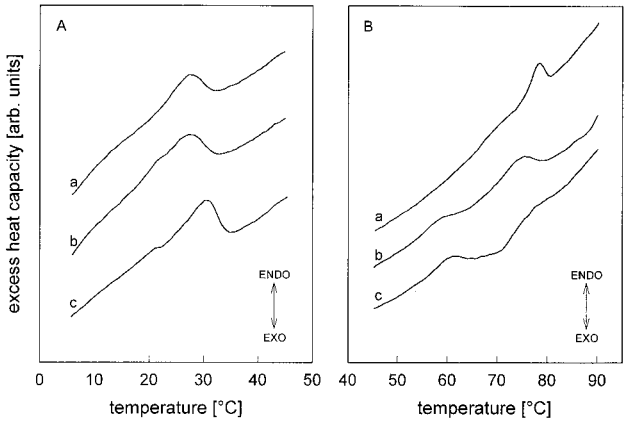

FIGURE 2: Excess heat capacity functions for LDL (a) and melittin-treated LDL [molar ratio of 10:1 (b) and 100:1 melittin:LDL (c)], after normalization to the scan rate and the amount of LDL. Panel A shows the reversible melting of the core-located cholesteryl esters and B the thermal unfolding of apoB-100.

Table 1: Increase in the Outer Hyperfine Splitting Constant (ΔA_{max}) of 5-DSA in LDL by Binding of Melittin to LDL at Different Molar Ratios

melittin/LDL (mol/mol)	ΔA_{max}[a] (G)		melittin/LDL (mol/mol)	ΔA_{max}[a] (G)	
	20 °C	37 °C		20 °C	37 °C
1	0.10	0.20	10	0.55	0.60
1	0.05	0.10	100	0.67	0.61
10	0.52	0.60	100	0.60	0.65

[a] Data for two independent preparations; the measurements were repeated twice.

LDL) led to a significant reduction of the transition temperature, $T_{m,protein}$, and broadening of the peak. In addition, a second, broad low-temperature transition at approximately 55 °C was observed, which became more pronounced when the melittin/LDL ratio was increased from 5 to 100 mol of melittin/mol of LDL. Concomitantly, the high-temperature transition vanished.

Electron Paramagnetic Resonance (EPR). The effect of melittin treatment on the phospholipid chain mobility was determined from the outer hyperfine splitting in the EPR spectra of the stearic acid spin-label with the active nitroxide group at either 5-C or 12-C. The spin-label was incorporated into the surface phospholipid monolayer of LDL with the carboxyl group at the surface and the fatty acid chain pointing toward the interior of the particle (*34*).

When melittin was added to LDL (1, 10, or 100 mol of melittin/mol of LDL), an increase in the maximum outer hyperfine splitting constant A_{max} was observed for 5-DSA (Table 1). For the stearic acid, spin-labeled at C-12 (12-DSA), no increase in A_{max} is detected. Melittin treatment of LDL thus caused a restriction of the phospholipid chain mobility near the phospholipid headgroups.

Copper-Mediated LDL Oxidation. Whenever LDL is oxidized under the conditions used in this study, usually three phases can be distinguished: (i) an inhibited phase in which Cu^{2+} is reduced to Cu^{+} by α-tocopherol and antioxidants are consumed (lag phase), followed by (ii) the propagation phase where the lipid peroxidation chain reaction leads to consumption of polyunsaturated fatty acids, accompanied by a rapid increase in the amount of conjugated dienes (CD) as the main initial oxidation products (these products decompose

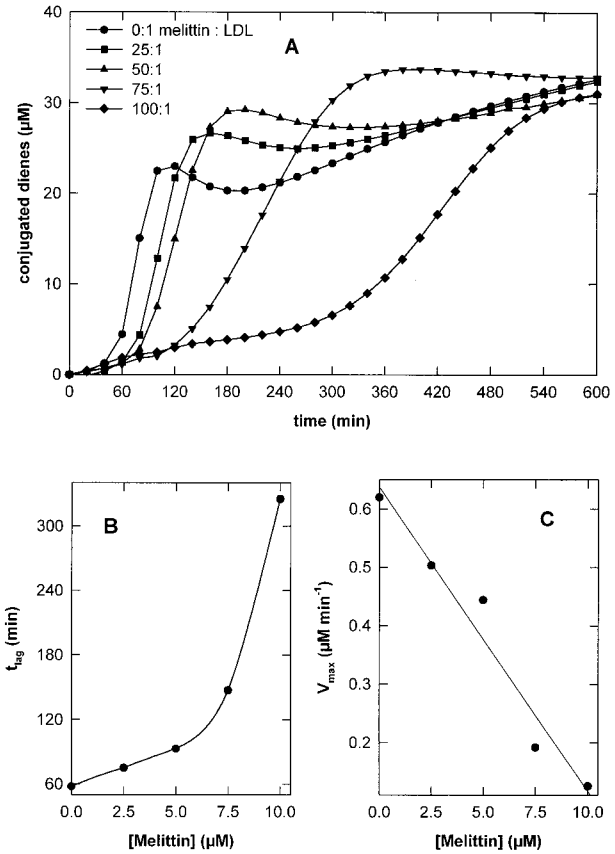

FIGURE 3: Effect of melittin on copper-mediated LDL oxidation. LDL (0.1 μM) was incubated with 1.6 μM Cu^{2+} in the presence of the melittin concentrations indicated, and formation of conjugated dienes was monitored at 234 nm. Panel A shows the typical time course of oxidation found at increasing melittin concentrations. Panel B shows plots of the dependence of lag time on melittin concentration, and panel C shows the change in maximum propagation rate as a function of melittin concentration.

subsequently, after the CD concentration has reached a maximum), and (iii) the decomposition phase, where CD hydroperoxides react further to give a wide variety of products.

LDL oxidation in the presence of melittin was largely hindered as shown in Figure 3; 0.1 μM LDL was incubated with increasing molar ratios of melittin (0−100 mol of melittin/mol of LDL) and oxidized with 1.6 μM Cu^{2+} (Figure 3A). Not only was the lag phase dramatically prolonged in a concentration-dependent fashion (58−325 min, Figure 3B), but the propagation rate also decreased accordingly (0.620−0.125 μM min^{-1}, Figure 3C). The latter indicates a reduction in the average rate of initiation, R_i, by about 45%, as R_i is proportional to the square of V_{max}. Additionally, the maximum amount of conjugated dienes formed (CD_{max}) increased significantly.

If this effect was solely due to copper chelation by melittin, increasing the copper concentration while keeping the melittin concentration constant would overcome the increase in lag time and the decrease in the propagation rate. The results of this experiment are shown in Figure 4; increasing copper concentrations (1.6−10 μM) did not affect the reduction of LDL oxidizability with respect to lag time, which remained essentially the same in the presence of melittin, irrespective of the copper concentration used. This indicates that the effect of melittin is not due to chelation,

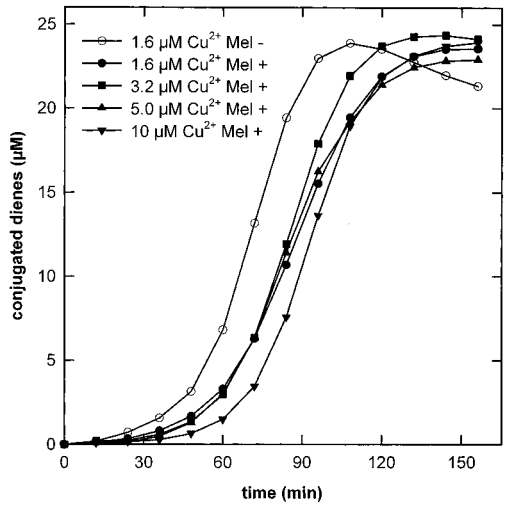

FIGURE 4: Effect of increasing copper concentrations in the presence of melittin. LDL was incubated with melittin at a molar ratio of 50:1, and oxidation was started by addition of the indicated concentration of Cu^{2+}. The lag time was increased as compared to the control (oxidation at 1.6 μM Cu^{2+} without melittin) and was not restored to the value of the control, even at very high copper concentrations, although the propagation rate reverted to some extent to the original value.

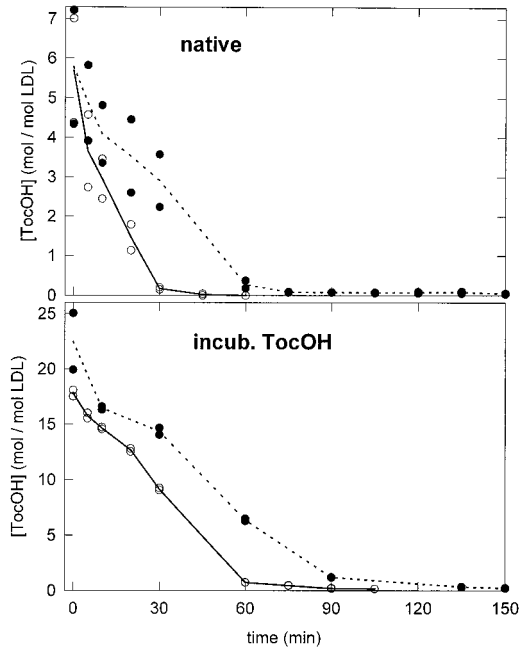

FIGURE 5: Consumption of antioxidants in the presence of melittin. α-Tocopherol was assayed during LDL oxidation (0.1 μM LDL and 1.6 μM Cu^{2+}) in the presence (100 mol of melittin/mol of LDL) and absence of melittin. In α-tocopherol-loaded LDL, α-tocopherol is consumed only marginally slower in the presence of melittin.

and that the copper concentration itself does not influence the action of melittin. CD_{max} was unchanged by increasing the copper concentration.

Figure 5 shows the time course of consumption of α-tocopherol during oxidation, in the absence and presence of 10 mol of melittin/mol of LDL. The top panel illustrates the effect of melittin in the case of native LDL; in the absence of melittin, α-tocopherol was consumed after 45 min, while the lag phase lasted for another 20 min after its consumption. In presence of melittin, however, the persistence of α-tocopherol in LDL was considerably prolonged, extending to

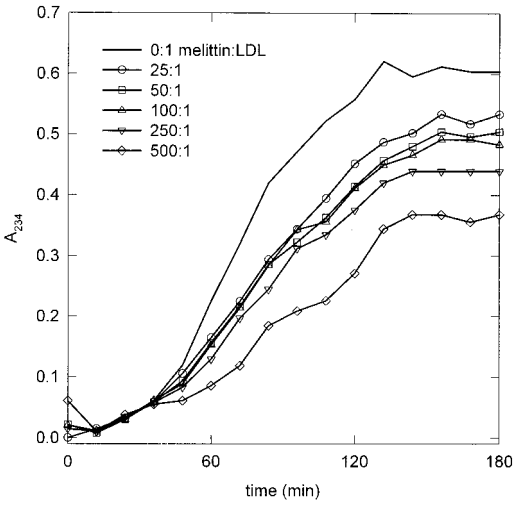

FIGURE 6: AAPH oxidation of LDL in the presence of melittin. LDL (0.1 μM) was oxidized with 1 mM AAPH in the presence of the indicated molar ratios of melittin, and formation of conjugated dienes was monitored at 234 nm.

about 120 min, with less than 1 mol/mol left after 75 min. Of the minor antioxidants, only γ-tocopherol showed a behavior similar to that of α-tocopherol (albeit it was consumed somewhat slower than α-tocopherol; data not shown); otherwise, minor antioxidants were consumed generally by the end of the lag phase in both cases (70 min in absence and 320 min in the presence of 10 μM melittin).

When LDL was loaded with α-tocopherol, the lag phase was generally longer than that for native LDL (120 min instead of 60 min), and in the presence of increasing melittin concentrations, the same principal behavior was observed with α-tocopherol-loaded LDL; i.e., increasing melittin concentrations increased the lag time and decreased V_{max} (not shown). However, consumption of α-tocopherol was not much slower in the presence of 100 mol of melittin/mol of LDL than in its absence (Figure 5, bottom panel). Actually, melittin was able to prolong the time required for consumption of α-tocopherol not longer than in native LDL, i.e., by about 30−40 min (based on the time where less than 1 mol/mol was left). It should be mentioned that at the high initial concentrations of α-tocopherol (23 mol/mol of LDL), γ-tocopherol appeared to be protected initially, and only after the α-tocopherol concentration had dropped below 50% of its initial value was γ-tocopherol rapidly consumed (not shown). Otherwise, consumption of γ-tocopherol was similar to that of α-tocopherol. Consumption of β-carotene was delayed in the presence of melittin, in both native and α-tocopherol-loaded LDL, but again decay of β-carotene was slower in α-tocopherol-loaded LDL, with only minimal consumption in the presence of α-tocopherol (not shown).

AAPH-Mediated LDL Oxidation. LDL (0.1 μM) was incubated a 37 °C with 1 mM AAPH, in absence and in the presence of increasing molar ratios of melittin (25−500 mol of melittin/mol of LDL). No significant effect of melittin on the lag phase was observed, but there was a decrease in the propagation rate, proportional to the melittin concentration (Figure 6).

Tryptophan Fluorescence Decay and Spectra. To monitor the effect of copper oxidation on protein damage in the presence and absence of melittin, we studied the changes in tryptophan fluorescence. As already described elsewhere

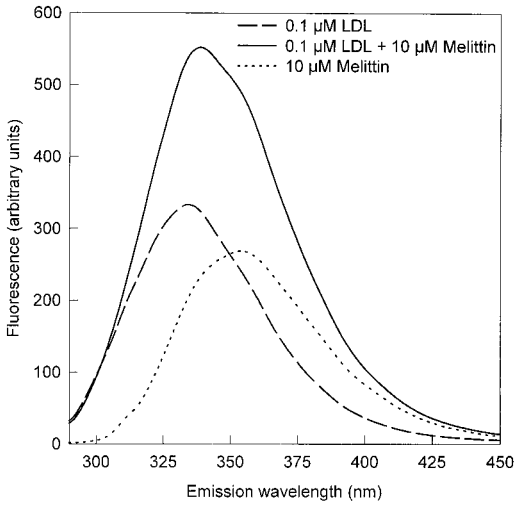

FIGURE 7: Tryptophan fluorescence of LDL and melittin. Tryptophan fluorescence was measured in PBS at 37 °C at the indicated molar ratios of LDL and melittin. The spectra of the constituents add up to the spectrum of the mixture of LDL and melittin.

(*16*), in the absence of melittin, after initial rapid quenching due to copper binding, tryptophan fluorescence decreased only slowly during the lag phase and then more rapidly during propagation, concomitant with LDL oxidation as monitored by measuring the formation of conjugated dienes. In presence of melittin, however, tryptophan fluorescence (both from the single Trp of melittin and from the 37 Trp's of LDL) did not change at all over 8 h of oxidation (not shown), although during this time formation of conjugated dienes is already observed (cf. Figure 3).

Superposition of the melittin and LDL fluorescence emission spectra yielded the spectrum of LDL and melittin (Figure 7), revealing that LDL-bound melittin shows no blue shift of tryptophan fluorescence maximum compared to that of free melittin and LDL in solution.

DISCUSSION

The Overall Integrity of the LDL Particle Is Maintained in the Presence of Melittin. From the SAXS data, it is readily concluded that at temperatures below the "core-melting" transition temperature, $T_{m,CE}$, the influence of melittin (100 mol/mol of LDL) is confined predominantly to the surface and leads to an increase in diameter, whereas the core regions remain essentially unaffected. The increase in particle size in the presence of melittin was more pronounced at temperatures above $T_{m,CE}$, and a considerable broadening of the maximum in $p(r)$ at large distances appeared, which corresponds to the electron density autocorrelation of phospholipid headgroups and protein (Figure 1D). This is consistent with some swelling and maybe aggregation of LDL particles. Above T_m, the changes in the interior of the LDL appear to be more pronounced. However, the overall integrity of LDL is preserved in the presence of melittin.

Effect of Melittin on the Conformation of ApoB-100. The most prominent change observed was the effect of melittin on thermally induced unfolding of apoB-100. Already at a low concentration of melittin (5 mol/mol of LDL), the high-temperature transition was shifted to lower temperatures, indicating a destabilization of apoB-100, with loss of conformational integrity. A second transition appeared at lower temperatures, which became more pronounced as the melittin concentration was increased. The action of melittin thus causes a segregation of the originally more or less uniformly unfolding domains of the protein into two populations with different thermal stabilities. This may be due to a modification of the interactions between protein and lipid resulting in an exposure of previously buried hydrophobic moieties of apoB-100 to the aqueous environment.

Furthermore, the characteristic time course of tryptophan fluorescence decay during oxidation (*16*) was completely abolished in the presence of melittin (not shown), indicating that both the initial fluorescence quenching due to copper binding (possibly by collision) and the subsequent oxidative destruction of tryptophan are prevented by melittin. On the other hand, there is still lipid peroxidation, albeit slower, and without apparent destruction of tryptophan residues. Further support for a preferential effect of melittin on apoB-100 is provided by the observation that the intensity and maximum of melittin fluorescence in the presence of LDL are unchanged compared to those of melittin alone (Figure 7). Moreover, the emission maximum of the single tryptophan of melittin indicates that tryptophan is located in a polar environment; obviously, neither the tryptophan residues on LDL nor the one on melittin showed a change of their respective environment upon binding of melittin, suggesting that the tryptophan located at position 19 of melittin is not deeply inserted into the hydrophobic part of the lipid monolayer but rather is located in the headgroup region of the phospholipids. This is in agreement with the observation that only 5-DSA spin-label shows an effect upon melittin binding, but not 12-DSA; the changes in the outer hyperfine splitting constants in the EPR spectra of 5-DSA in the presence of melittin indicate a reduced mobility of the phospholipids' acyl chains in the vicinity of the headgroup.

The Action of Melittin on the ApoB-100 Conformation Leads to Separation of Redox-Active Copper and α-Tocopherol. Melittin was able to hinder copper-mediated lipid peroxidation in LDL considerably already at rather low concentrations. Although there was still lipid peroxidation at a lower rate, copper-induced quenching of tryptophan fluorescence was completely abolished in the presence of melittin, and lipid peroxidation was not accompanied by destruction of tryptophan residues, a process which, in the absence of melittin, parallels the extent and time course of lipid peroxidation (*16*). This indicates prevention of copper binding near tryptophan residues, and in combination with the strongly reduced oxidizability of LDL, suggests an important role of tryptophan-containing Cu^{2+}-binding sites.

The action of melittin on LDL is not that of a chain-breaking antioxidant, like α-tocopherol, as it acted both during the lag phase and during propagation which indicates that it is not consumed like a reductant would be. Also, as evident from Figure 5, melittin could not prevent consumption of α-tocopherol; it only retarded it. Neither is the action of melittin explained by a mere redox inactivation through chelation of copper ions, because increasing copper concentrations, even to very high levels, did not significantly reduce the lag time or increase the propagation rate. Both observations together suggest that melittin strongly affects the interaction of protein-bound copper with α-tocopherol, the reaction in which the primordial radicals responsible for the initiation of LDL oxidation are generated (*9*). This blocking

of the interaction, which most likely involves protein-related copper-binding sites, is not reversible. This is also reflected by a very slow consumption of α-tocopherol, extending over the whole lag phase, implying that its role is limited to an antioxidant effect in the presence of melittin, such as in AAPH-mediated oxidation.

It has been pointed out by Lynch and Frei (*35*) that copper is reduced preferentially by α-tocopherol, when added to LDL. This suggests a very specific interaction of copper and α-tocopherol which appears to be mediated by apoB-100, probably by binding sites in the vicinity of tryptophan (*16*). However, conformational changes of apoB-100 brought about by melittin might prevent proper binding of Cu^{2+} to these sites, abolishing the specific interaction with α-tocopherol. As a consequence, there is only nonspecific copper binding, resulting in slow LDL oxidation by a different mechanism which does not involve protein-bound Cu^{2+}.

It is shown in this study that melittin affects also AAPH-mediated LDL oxidation (Figure 7). Although the lag time is practically unaffected, a decrease of the propagation rate proportional to the melittin concentration was observed, similar to the decrease in the rate of copper-mediated oxidation. A possible explanation for this effect is that the mobility or packing density of LDL lipids is changed due to the intercalation of melittin between apoB-100 and the lipid. This would indicate a considerable general influence of apoB-100 on the oxidizability of LDL in addition to the more specific effect on copper−tocopherol interactions.

Uncoupling of α-Tocopherol and Initiation of Lipid Peroxidation. It has been shown both experimentally and by simulation studies (*8*, *9*, *35*) that copper reduction by α-tocopherol plays a very important role in the initiation of LDL oxidation. By reduction of Cu^{2+}, α-tocopherol is converted to α-tocopheroxyl radical which is the first initiating species, provided no hydroperoxide is present (*9*). Alternatively, reduction equivalents might be provided otherwise, e.g., by apoB-100, leading to directly initiating radicals (*36*). When the similarly reduced propagation rates are considered, it appears that melittin in fact reduces the oxidizability of the lipid moiety of LDL, very likely by modifying the lipid−protein interactions of apoB-100 which would affect the conformational state of both the lipid and protein. It is conceivable that this conformational change does not merely lead to a reduced ability to bind copper but that the close interaction between the copper-binding site and the lipid or α-tocopherol loosens, thus reducing the rate of primordial radical formation by "uncoupling" the reduction of copper and the oxidation of α-tocopherol. This is supported by the notion that the coupled redox cycle of copper and α-tocopherol is the driving force of initiation of lipid peroxidation in native LDL and that apoB-100 plays an important role not only in binding copper but also in aiding in the solubilization of it in the lipid moiety. Rather, in native LDL containing only six or seven molecules of α-tocopherol, it appears to be usually located close to protein-bound copper, and it can be regarded at least as a striking coincidence that seven or eight tryptophan residues out of 37 are accessible to interactions with Cu^{2+} ions (*16*). Also, it can be observed that in the presence of melittin, "minor" antioxidants are ineffective, although they can normally prolong the lag time considerably (*9*), indicating that predominant copper reduction by α-tocopherol has been replaced by a mechanism which does not induce large variations in the rate of initiation, like the reduction of copper by α-tocopherol. On the other hand, this also explains why increasing α-tocopherol concentrations can indeed render LDL more resistant to oxidation although a substantial fraction of the antioxidant present on "normal" LDL is clearly involved in the reduction of Cu^{2+} (*37*) and thus a prooxidant; such α-tocopherol molecules on LDL which are not located close to copper-binding sites can only act as antioxidants, and this fraction is bound to increase whenever LDL is loaded with tocopherol.

A close inspection of the results obtained in this work in light of the proposed mechanism of copper-mediated LDL oxidation (*9*) leads to the conclusion that, whenever α-tocopherol is involved in copper-reduction, two effects are the consequence; larger amounts of α-tocopherol on LDL would increase the rate of copper reduction, but also would be more efficient in radical scavenging. A colocalization of prooxidant transition metal ions and α-tocopherol on LDL would mean that the natural amount of α-tocopherol on LDL may be just sufficient to balance the prooxidant and antioxidant properties as described in ref *9*. However, an excess of the vitamin can lead to an increased radical scavenging effect, thus tipping the scales to the antioxidant.

ACKNOWLEDGMENT

Dedicated to the memory of Prof. Dr. Hermann Esterbauer. The technical assistance of Ms. Gerhild Harter and Ing. Monika Zechner is gratefully acknowledged.

REFERENCES

1. Halliwell, B., and Gutteridge, J. M. C. (1990) Role of Free Radicals and Catalytic Metal Ions in Human Disease: an Overview, *Methods Enzymol. 186*, 1−88.
2. Esterbauer, H., and Ramos, P. (1995) Chemistry and Pathophysiology of Oxidation of LDL, *Rev. Physiol. Pharmacol. 127*, 31−64.
3. Kostner, G. M., and Laggner, P. (1989) in *Human Plasma Lipoproteins: Clinical Biochemistry, Principles Methods, Applications 3* (Fruchard, J. C., and Shepherd, J., Eds.) pp 23−54, W. de Gruyter, Berlin and New York.
4. Laggner, P. (1995) in *Modern Aspects of Small-Angle Scattering* (Brumberger, H., Ed.) pp 371−386, Kluwer, Dordrecht, The Netherlands.
5. Deckelbaum, R. J., Shipley, G. G., Small, D. M., Lees, R. S., and George, P. K. (1975) *Science 190*, 392−394.
6. Atkinson, D., Deckelbaum, R. J., Small, D. M., and Shipley, G. G. (1977) *Proc. Natl. Acad. Sci. U.S.A. 74*, 1042−1046.
7. Laggner, P., and Müller, K. (1978) *Q. Rev. Biophys. 11*, 371−425.
8. Kontush, A., Meyer, S., Finckh, B., Kohlschütter, A., and Beisiegel, U. (1995) *J. Biol. Chem. 271*, 11106−11112.
9. Abuja, P. M., Albertini, R., and Esterbauer, H. (1997) *Chem. Res. Toxicol. 10*, 644−651.
10. Knott, T. J., Pease, R. J., Powell, L. M., Wallis, S. C., Rall, S. C., Jr., Innerarity, T. L., Blackhart, B., Taylor, W. H., Marcel, Y., Milne, R., Johnson, D., Fuller, M., Lusis, A. J., McCarthy, B. J., Mahley, R. W., Levy-Wilson, B., and Scott, J. (1986) *Nature 323*, 734−738.
11. Yang, C.-Y., Chen, S.-H., Gianturco, S. H., Bradley, W. A., Sparrow, J. T., Tanimura, M., Li, W.-H., Sparrow, D. A., DeLoof, H., Rosseneu, M., Lee, F.-S., Gu, Z.-W., Gotto, A. M., Jr., and Chan, L. (1986) *Nature 323*, 738−742.
12. Sommer, A., Prenner, E., Gorges, R., Stütz, H., Grillhofer, H., Kostner, G. M., Paltauf, F., and Hermetter, A. (1992) *J. Biol. Chem. 267*, 24217−24222.

13. Segrest, J. P., Jones, M. K., Mishra, V. K., Anantharamaiah, G. M., and Garber, D. W. (1994) *Arterioscler. Thromb. 14*, 1674−1685.
14. Gieseg, S. P., and Esterbauer, H. (1994) *FEBS Lett. 343*, 188−194.
15. Prassl, R., Schuster, B., Laggner, P., Flamant, C., Nigon, F., and Chapman, M. J. (1998) *Biochemistry 37*, 938−944.
16. Giessauf, A., Steiner, E., and Esterbauer, H. (1995) *Biochim. Biophys. Acta 1256*, 221−232.
17. Ferguson, E., Singh, R. J., Hogg, N., and Kalyanaraman, B. (1997) *Arch. Biochem. Biophys. 341*, 287−294.
18. Hoff, H. F., and Hoppe, G. (1995) *Curr. Opin. Lipidol. 6*, 317−325.
19. Camejo, G., Hurt, E., Wiklund, O., Rosengren, B., López, F., and Bondjers, G. (1991) *Biochim. Biophys. Acta 1096*, 253−261.
20. Kritharides, L., Jessup, W., and Dean, R. (1995) *Arch. Biochem. Biophys. 323*, 127−136.
21. Ehrenwald, E., Chisolm, G. M., and Fox, P. L. (1994) *J. Clin. Invest. 93*, 1493−1501.
22. Lamb, D. J., and Leake, D. S. (1994) *FEBS Lett. 338*, 122−126.
23. Swain, J. A., Darley-Usmar, V., and Gutteridge, J. M. C. (1994) *FEBS Lett. 342*, 49−52.
24. Ehrenwald, E., and Fox, P. L. (1996) *J. Clin. Invest. 97*, 884−890.
25. Maggi, E., Chiesa, R., Melissano, G., Castellano, R., Astore, D., Grossi, A., Finardi, G., and Bellomo, G. (1994) *Atheroscler. Thromb. 14*, 1892−1899.
26. Lohner, K., and Epand, R. (1997) *Adv. Biophys. Chem. 6*, 53−66.
27. Lund-Katz, S., Phillips, M. C., Mishra, V. K., Segrest, J. P., and Anantharamaiah, G. M. (1995) *Biochemistry 34*, 9219−9236.
28. Ramos, P., Gieseg, S. P., Schuster, B., and Esterbauer, H. (1995) *J. Lipid Res. 36*, 2113−2129.
29. Puhl, H., Waeg, G., and Esterbauer, H. (1993) *Methods Enzymol. 233*, 425−441.
30. Glatter, O. (1977) *J. Appl. Crystallogr. 10*, 415−421.
31. Müller, K., Laggner, P., Glatter, O., and Kostner, G. M. (1978) *Eur. J. Biochem. 82*, 73−80.
32. Gallová, J., Abuja, P. M., Pregetter, M., Laggner, P., and Prassl, R. (1998) *Chem. Phys. Lipids* (in press).
33. Deckelbaum, R. J., Shipley, G. G., and Small, D. M. (1977) *J. Biol. Chem. 252*, 744−754.
34. Kveder, M., Pifat, G., Pecar, S., and Schara, M. (1994) *Chem. Phys. Lipids 70*, 101−108.
35. Lynch, S. M., and Frei, B. (1995) *J. Biol. Chem. 270*, 5158−5163.
36. Davies, M. J., Fu, S., and Dean, R. T. (1995) *Biochem. J. 305*, 643−649.
37. Perugini, C., Seccia, M., Bagnati, M., Cau, C., Albano, E., and Bellomo, G. (1998) *Free Radical Biol. Med. 25*, 519−528.

BI981592P